

Article

Advancing Crop Yield Predictions: AQUACROP Model Application in Poland's JECAM Fields

Ewa Panek-Chwastyk ^{*}, Ceren Nisanur Ozbilge , Katarzyna Dąbrowska-Zielińska and Radosław Gurdak 

Remote Sensing Centre, Institute of Geodesy and Cartography, 02-679 Warsaw, Poland; katarzyna.dabrowska-zielinska@igik.edu.pl (K.D.-Z.); radoslaw.gurdak@polsa.gov.pl (R.G.)

* Correspondence: ewa.panek@igik.edu.pl

Abstract: This study, employing the AquaCrop model, demonstrated notable efficacy in assessing and predicting crop yields for winter wheat, maize, winter rapeseed, and sugar beets in the Joint Experiment for Crop Assessment and Monitoring (JECAM) test area of Poland from 2018 to 2023. In-situ measurements, conducted through field campaigns, included parameters such as electromagnetic radiation reflectance, Leaf Area Index (LAI), soil moisture, accumulated photosynthetically active radiation, chlorophyll content, and plant development phase. The model was calibrated with input data covering daily climatic parameters from the ERA5-land Daily Aggregated repository, crop details, and soil characteristics. Specifically, for winter wheat, the Root Mean Square Error (RMSE) values ranged from 1.92% to 14.26% of the mean yield per hectare. Maize cultivation showed RMSE values ranging from 0.21% to 1.41% of the mean yield per hectare. Winter rapeseed exhibited RMSE values ranging from 0.58% to 17.15% of the mean yield per hectare. In the case of sugar beets, the RMSE values ranged from 0.40% to 1.65% of the mean yield per hectare. Normalized Difference Vegetation Index (NDVI)-based predictions showed higher accuracy for winter wheat, similar accuracy for maize and sugar beets, but lower accuracy for winter rapeseed compared to Leaf Area Index (LAI). The study contributes valuable insights into agricultural management practices and facilitates decision-making processes for farmers in the region.

Keywords: AquaCrop; in-situ measurements; NDVI; yield prediction; croplands; sustainable agriculture



Citation: Panek-Chwastyk, E.; Ozbilge, C.N.; Dąbrowska-Zielińska, K.; Gurdak, R. Advancing Crop Yield Predictions: AQUACROP Model Application in Poland's JECAM Fields. *Agronomy* **2024**, *14*, 854. <https://doi.org/10.3390/agronomy14040854>

Academic Editor: Gniewko Niedbała

Received: 29 March 2024

Revised: 12 April 2024

Accepted: 18 April 2024

Published: 19 April 2024



Copyright: © 2024 by the authors. Licensee MDPI, Basel, Switzerland. This article is an open access article distributed under the terms and conditions of the Creative Commons Attribution (CC BY) license (<https://creativecommons.org/licenses/by/4.0/>).

1. Introduction

The agricultural study conducted in Wielkopolska, situated in central-west Poland, holds significance against the backdrop of the region's recent susceptibility to drought conditions. In particular, this region has experienced a heightened vulnerability to dry spells in recent years [1]. Given the climatic challenges posed by these conditions, monitoring and assessing crop growth has become paramount in this part of Poland.

The historical significance of the tested region in Poland as one of the primary agricultural hubs adds depth to its contemporary agricultural challenges. Over the years, Wielkopolska has consistently held a prominent position as one of the main agricultural regions in the country [2]. The rich agricultural heritage of this region has contributed significantly to Poland's agricultural landscape.

Wielkopolska, characterized by a warm, humid continental climate [3], faces the intricate task of sustaining various crops, including winter wheat, winter rapeseed, maize, and sugar beet. The region's reliance on rainfed agriculture, combined with evolving climate patterns, underscores the need for a comprehensive understanding of crop dynamics and environmental interactions.

While several recognized models, such as APSIM, DSSAT, EPIC, ALMANAC, and CropSyst, alongside studies correlating satellite data with crop yield, simulate crop growth based on physiological responses to environmental factors [4–9], the decision to employ the AquaCrop model in this study stems from its concurrent testing on maize fields in

Africa as part of the “SA Polish collaborative crop growth monitoring and yield assessment system for early warning utilizing new satellite Earth Observations data from Copernicus Program” (SAPOL) project. Given the project’s focus on assessing the model’s performance under drought conditions, the authors sought to evaluate its applicability in the context of drought susceptibility in Wielkopolska, Poland. This unique opportunity allowed for a comparative analysis of AquaCrop’s effectiveness across diverse agricultural settings, providing valuable insights into its potential utility under varying climatic conditions. Existing models often involve extensive numerical datasets, and require appropriate calibration, making them complex, especially for end-users like farmers [10]. The AquaCrop model, devised by the Food and Agriculture Organization (FAO), serves as a farm-level simulation tool specifically designed to address these challenges. It aims to simulate various irrigation scenarios and estimate crop canopy cover, biomass, and final yield [11]. Its balanced combination of simplicity, accuracy, and robustness makes it an optimal solution for irrigation strategies in diverse climatic environments [12]. The integration of in-situ measurements, conducted within the Joint Experiment for Crop Assessment and Monitoring (JECAM) area, becomes pivotal in providing real-time data for the calibration and validation of the AquaCrop model.

Notably, JECAM’s field campaigns, spanning from 2018 to 2023, have been strategically timed to align with meteorological conditions. This approach ensures the vigilant monitoring of crop variability, especially in the face of the heightened risk of drought in the Wielkopolska region. The selection of key crops, including winter wheat, winter rapeseed, maize, and sugar beet, provides a representative sample for detailed monitoring during the vegetation season.

The methodology encompasses a suite of in-situ measurements, capturing parameters such as electromagnetic radiation reflectance, Leaf Area Index (LAI), soil moisture, photosynthetically active radiation, chlorophyll content, plant development phases, and plant height. The geographical coordinates of the monitored fields are precisely recorded using GPS receivers, facilitating spatial referencing for subsequent analyses.

Importantly, this article underscores that the value of the study goes beyond the application of the AquaCrop model for yield prediction and sustainable agriculture. Its key aspects include the utilization of not only in-situ data collected during field campaigns or by farmers, as well as the integration of high-resolution satellite data from the Copernicus Land Monitoring Service, sourced from the Sentinel-2 satellite. This approach minimizes personal intervention by farmers in the fields and has proven crucial in today’s era for the advancement of precision agriculture.

The AquaCrop model, at the core of this study, operates as a planning tool to support management decisions in rainfed agriculture. Given Wielkopolska’s susceptibility to drought, the model’s ability to simulate the growth and yield of crops becomes invaluable. The study also emphasizes the AquaCrop model’s versatility in considering atmospheric conditions, soil characteristics, and field management components.

As a region exposed to the challenges of changing climate patterns, Wielkopolska’s agricultural landscape necessitates a robust monitoring system. The AquaCrop model, integrated with in-situ measurements and tailored for the specific conditions of the JECAM area in Wielkopolska, emerges as a crucial tool in understanding and predicting crop performance. This article delves into the detailed materials, methods, and data processing techniques employed in this study, shedding light on the intricate interplay between agriculture, climate, and technology in the context of the Wielkopolska region’s agricultural resilience.

2. Materials and Methods

The AquaCrop model was utilized to evaluate and forecast crop yields for winter wheat, maize, winter rapeseed, and sugar beets in the central-west region of Poland (Figure 1). Files necessary for each crop type were parameterized, calibrated, and validated using ERA-5 climate data, in-situ soil, and plant phenology data [13]. Following the

calibration and validation phase, in-situ Leaf Area Index (LAI) measurements obtained using the LAI-2200C Plant Canopy Analyzer and satellite Sentinel-2 Normalized Difference Vegetation Index (NDVI)-based simulations were conducted for the four different crop types between 2018 and 2023. As part of this extensive study, we rigorously tested the AquaCrop model over six years, from 2018 to 2023, monitoring agrometeorological conditions from sowing to the end of the vegetative season. This finely tuned model, based on six years of data, will be employed to forecast yields in the forthcoming years and will undergo further validation by end-users. Various statistical analyses, including on metrics such as Root Mean Square Error (RMSE), Mean Absolute Error (MAE), and Mean Absolute Percentage Error (MAPE), were utilized to evaluate the accuracy of the obtained yield values and simulation results.

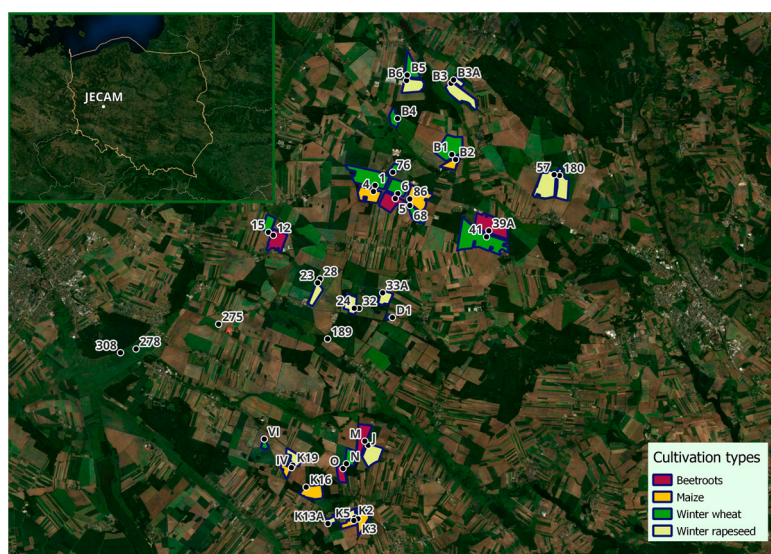


Figure 1. Sampling points' distribution in the JECAM tested area and cultivation types for the tested year 2018.

2.1. In-Situ Measurements

The field site, covering an area of 25 km × 25 km, underwent meticulous planning of cultivation and harvesting schedules for various crops from 2018 to 2023. This planning aimed to synchronize with the specific requirements of each crop type and the prevailing meteorological conditions. Winter wheat, sown in September and harvested in August, underwent its growth cycle during the cooler months, while maize, planted in mid-April and harvested in November, thrived during the warmer seasons. Sugar beet, sown in early April and harvested in November, followed a growth pattern similar to maize. Rapeseed, sown at the end of August and harvested in mid-August of the following year, had a longer growth period extending over two seasons.

These cultivation and harvesting timelines were synchronized with the JECAM field campaigns, conducted from April, marking the onset of the vegetation season, until early July. The selection of 42 fields during the initial campaign formed the basis for the continuous monitoring of plant conditions throughout the growth period, covering each vegetation season over the span of six years. These fields comprised 15 winter wheat fields, 12 rapeseed fields, 10 maize fields, and 5 sugar beet fields. The geographical coordinates of the selected points were recorded using GPS receivers, facilitating precise spatial referencing for subsequent analyses. The distribution of the measurement fields within the JECAM area in the Wielkopolska Voivodeship is illustrated in Figure 1.

During each campaign, a suite of parameters was measured to comprehensively assess the physiological and environmental aspects of the selected crops. The measured parameters included electromagnetic radiation reflectance using ASD FieldSpec 4 Hi-Res (Malvern Panalytical, Malvern, UK) (depending on weather conditions), LAI using the LAI-2200C

Plant Canopy Analyzer (LI-COR, Lincoln, NE, USA), soil moisture using TRIME PICO (IMKO Micromodultechnik GmbH, Ettlingen, Germany), accumulated photosynthetically active radiation using AccuPar, chlorophyll content using FieldScout CM 1000 Chlorophyll Meter (Spectrum Technologies, Aurora, IL, USA), plant development phase, and plant height.

Simultaneously, samples of each observed crop type were collected, with each sample covering an area of 1 m². Subsequently, laboratory measurements were conducted, including fresh biomass weight, dry biomass weight, water content in plants, 250-grain weight, and 1000-grain weight. Additionally, during the sample harvesting process, the number of plants within the 1 m² frame and the quantity of spikes were recorded. The meticulously measured parameters played a crucial role in determining the in-situ yield per hectare (t·ha⁻¹) for each wheat field. It is worth noting that, for wheat, samples were collected for each field in each of the six test years to determine the yield from each measurement point, whereas for the other crops, the yield was determined as the average yield from all cultivated plots specifically for that crop within the studied region.

The selection of these parameters aimed to capture a holistic understanding of crop health, growth dynamics, and environmental interactions.

2.2. AQUACROP Model Overview

The software AquaCrop (Version: 7.0, Manufacturer Name: Food and Agriculture Organization of the United Nations (FAO), City: Rome, Country: Italy), developed by the FAO's Land and Water Division, aims to enhance water-efficient agricultural methods [14]. This approach utilizes the water balance concept to integrate soil, plant, and atmospheric components [15]. To simulate the growth and yield of agricultural products, AquaCrop considers various factors including atmospheric conditions (such as precipitation, temperature, evapotranspiration, and carbon dioxide concentration), physical and hydraulic processes of soil (including soil profile and groundwater characteristics), plant physiological and productivity parameters (such as phenology, crop cover, rooting depth, biomass production, and harvestable yield), as well as field management practices (including irrigation and field cultivation techniques) [16].

The simulation process comprises four stages, executed consecutively at every time step of the day, involving the following calculations [17].

The first step involves the development of canopy cover. AquaCrop indicates foliage growth using green (canopy cover) (CC), indicating the proportion of the soil surface covered by green canopy:

$$CC = \frac{\text{soil surface covered by the green canopy}}{\text{unit ground surface area}} \quad (1)$$

Crop transpiration is calculated by multiplying the reference evapotranspiration (ET_o) by the crop transpiration coefficient (K_{CTr}) and a water stress coefficient (K_s) [18]:

$$T_r = K_s K_{CTr} ET_o \quad (2)$$

This coefficient is equal to 1 when water stress does not induce stomatal closure.

The crop transpiration coefficient (K_{CTr}) is proportional to the green canopy cover (CC):

$$K_{CTr} = K_{CTr,x} CC^* \quad (3)$$

where CC* is the canopy cover adjusted for micro-advective effects, and K_{CTr,x} is the crop coefficient for maximum crop transpiration, which is determined by the characteristics distinguishing a crop with full canopy cover from reference grass. Typically, K_{CTr,x} varies between 1.05 and 1.20 for most crops [18].

The total biomass (B) is calculated by the model using normalized water productivity (WP) and the cumulative crop transpiration over the growing season as follows:

$$B = WP * \sum Tr \quad (4)$$

Through the utilization of parameter B and the harvest index (HI), one can determine the harvestable yield (Y) from [19]:

$$Y = HI * B \quad (5)$$

AquaCrop provides a yield value by converting the daily simulated crop transpiration into equivalent biomass, which is then subsequently translated into yield using harvest index values [20].

The model is designed to serve as a planning tool to support management decisions in both rainfed and irrigated agriculture, used by practitioners employed in extension services, government agencies, non-governmental organizations, and farmer associations. It is also employed as a tool to examine how water affects crop productivity [21].

2.3. Data Processing Methodology

This section provides details regarding the methodology (Figure 2) used for acquiring predictive data based on the AquaCrop model and input data obtained from various sources.

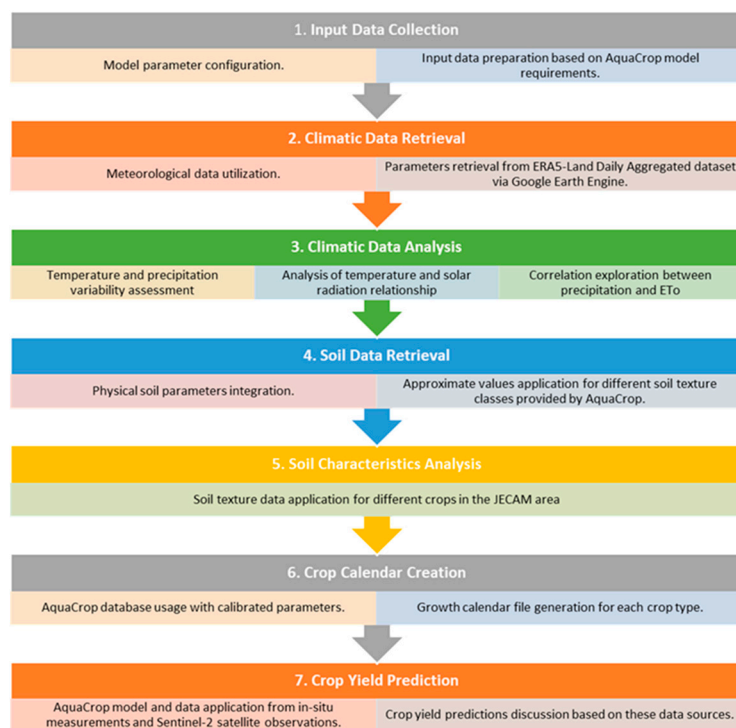


Figure 2. Schematic representation of AquaCrop model workflow and data interactions in the study.

2.3.1. Required Input Data

The AquaCrop model requires climatic parameters, crop information, soil characteristics, field management, and irrigation [22]. It is essential to emphasize that this model comprises a comprehensive set of input parameters, allowing the adjustment of relevant factors to the soil type in the JECAM area and the type of cultivation, particularly concerning meteorological conditions. Weather, crop, soil, and test area data were prepared in accordance with AquaCrop input data requirements.

2.3.2. Climatic Data

The reference crop evapotranspiration (ET_o) is calculated within the model using the provided meteorological data, including minimum (T_n) and maximum (T_x) air temperature, dew point temperature (T_{dew}), wind speed at x meters above the soil surface (u(x)), solar or shortwave radiation (R_s), and rainfall. These data are obtained from the ERA5-Land Daily Aggregated dataset with a resolution of 9 km through the Google Earth Engine platform.

The relationship between precipitation and ET_o (reference evapotranspiration) throughout the simulation period is presented in Figure 3. The overall trend of the graph indicates significantly higher levels of precipitation and ET_o during summer months, while these values noticeably decrease in winter months.

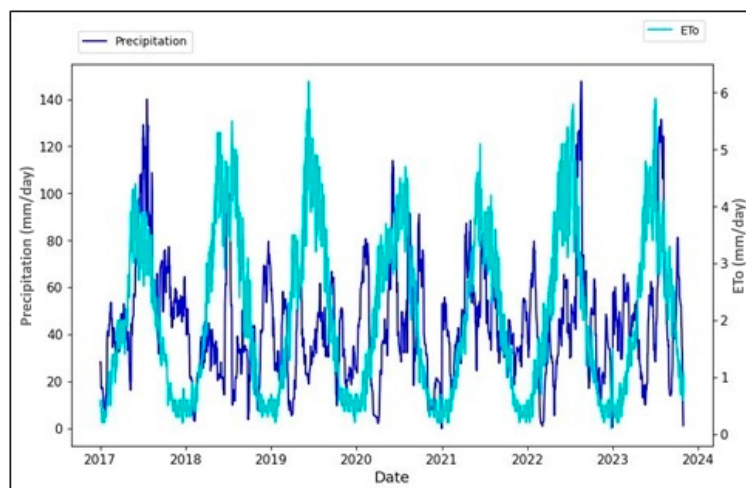


Figure 3. Daily values of atmospheric precipitation and ET_o for the years 2018–2023.

In the context of the AquaCrop model, evapotranspiration is a complex process that involves the evaporation of water from the soil surface and plant transpiration. This process is sensitive to various factors such as atmospheric conditions, biological characteristics of the plant, crop management, and environmental variables. Evapotranspiration from the reference surface, also known as reference evapotranspiration (ET_o), is a key parameter in the AquaCrop model. ET_o represents the amount of water evaporated from the reference plant surface.

The FAO Penman–Monteith method is used to calculate ET_o in accordance with the calculation procedures described in FAO Irrigation and Drainage paper Nr. 56. [23], which takes into account various variables such as air temperature, air humidity, wind speed, and solar radiation. This equation allows the precise determination of the rate of evapotranspiration based on available meteorological data.

Data such as air humidity, solar radiation, air temperature, and wind speed necessary for calculating ET_o were also obtained from the ERA5-Land Daily Aggregated dataset through the Google Earth Engine platform.

AquaCrop employs a reference atmospheric CO₂ concentration of 369.41 parts per million by volume (ppm), representing the average CO₂ concentration for the year 2000 at Mauna Loa Observatory. This specific value is crucial for normalizing the biomass water productivity (WP) in the model. The normalization for atmospheric CO₂ involves adjusting the WP to account for variations in CO₂ concentration. This adjustment is necessary because crop is influenced by atmospheric CO₂ levels, and AquaCrop aims to provide accurate simulations by considering conditions at the reference location [24].

2.3.3. Soil Profile Characteristics

The AquaCrop model incorporates essential physical soil parameters to calculate water content in the root zone (W_r) and simulate soil water flow. This involves a comprehensive

soil water balance that monitors daily water transfers, including inputs such as rainfall, irrigation, and capillary rise, and outputs such as percolation and evapotranspiration [25]. AquaCrop's soil profile consists of various soil horizons, each characterized by distinct physical properties [26]. When local measurements of soil characteristics are unavailable, AquaCrop provides default values for different Soil Texture Classes [23]. To ensure consistent model initialization, specific Soil Texture Classes for different crops were used, as presented in Table 1. For example, winter wheat was associated with a clay loam Soil Texture Class. Corresponding values for Soil Water Content (θ), Total Available Water (TAW), and Saturated Hydraulic Conductivity (Ksat) were derived from AquaCrop's default values for this Soil Texture Class. This practice ensures that the model starts with similar initial soil moisture conditions across various simulations, enabling a more controlled assessment of model performance or the impact of different factors on soil moisture during the simulation period.

Table 1. Soil textural classes for different crops in the JECAM area.

Crop Types	Soil Textural Class	Soil Water Content (θ)			TAW	Ksat
		SAT (vol %)	FC (vol %)	PWP (vol %)	(mm/m)	(mm/day)
Winter wheat	clay loam	50	39	23	160	125
Maize	loam	46	31	15	160	500
Sugar beet	loam	46	31	15	160	500
Winter rapeseed	clay loam	50	39	23	160	125

Where SAT is saturated soil moisture level, which indicates when the entire pore space is filled with water; FC represents the maximum amount of water retained by well-drained soil against gravitational forces, available to plants; Permanent Wilting Point (PWP) is the soil water content at which plants cease to take up water and permanently wilt; Saturated Hydraulic Conductivity (Ksat) refers to how hydraulic conductivity determines the soil's ability to conduct water. In saturated soil, all pores are filled with water, and the hydraulic conductivity value reaches its maximum value. TAW is total available soil water, calculated for soil water balance. TAW is derived from the water characteristics of the soil's fine fraction and gravel content [24].

2.3.4. Crop Calendar

For each type of crop studied, a cultivation characteristics file was created, specifying dates from day 1 after sowing to adjust the growth stages to specific crops and properly calibrate the model to prevailing conditions in western Poland.

2.3.5. Crop Yield Prediction

To forecast crop yields, the study utilized the AquaCrop model, incorporating data derived from both in-situ LAI measurements and satellite observations facilitated by the Sentinel-2 satellite constellation.

A pivotal component of satellite data processing involved implementing the NDVI as a crucial parameter within the AquaCrop model. The NDVI computation utilized specific spectral channels from Sentinel-2, including the Red and Near-Infrared bands, with the formula:

$$\text{NDVI} = \frac{(\text{NIR} + \text{Red})}{(\text{NIR} - \text{Red})} \quad (6)$$

The integration of NDVI served as a cornerstone in computing canopy cover (CC), a parameter responsible for quantifying the fraction of the soil surface covered by the canopy.

Efforts were made to mitigate the impact of clouds on the accuracy of derived values. Cloud masking involved using the Sentinel-2 Quality Assessment (QA) band, specifically excluding pixels identified as cloudy in the QA band with a threshold below 10%, ensuring a rigorous selection process for accurate NDVI computation. This process ensured that computed NDVI values accurately represented vegetation status by filtering out interference caused by cloud cover.

In this study, two parallel simulations were conducted using the AquaCrop model. In the first scenario, in-situ LAI measurements were utilized instead of canopy cover, while in

the second scenario, satellite-derived NDVI was employed. This dual approach allowed for a comprehensive assessment, providing insights into the model’s performance under different data sources, namely, in-situ and satellite-based measurements.

3. Results

3.1. Winter Wheat Yield Predictions

Figure 4 presents a comparison between simulated and observed yields for winter wheat crops from 2018 to 2023. The simulation results for winter wheat in 2020 show relatively lower sensitivity, with an RMSE of 1.45 t·ha⁻¹ (see Table 2). These results significantly deviate from actual values, indicating reduced reliability compared to other years. Conversely, in 2023, with an RMSE of 0.1 t·ha⁻¹, the simulation closely approximates measured values, providing more dependable outputs.

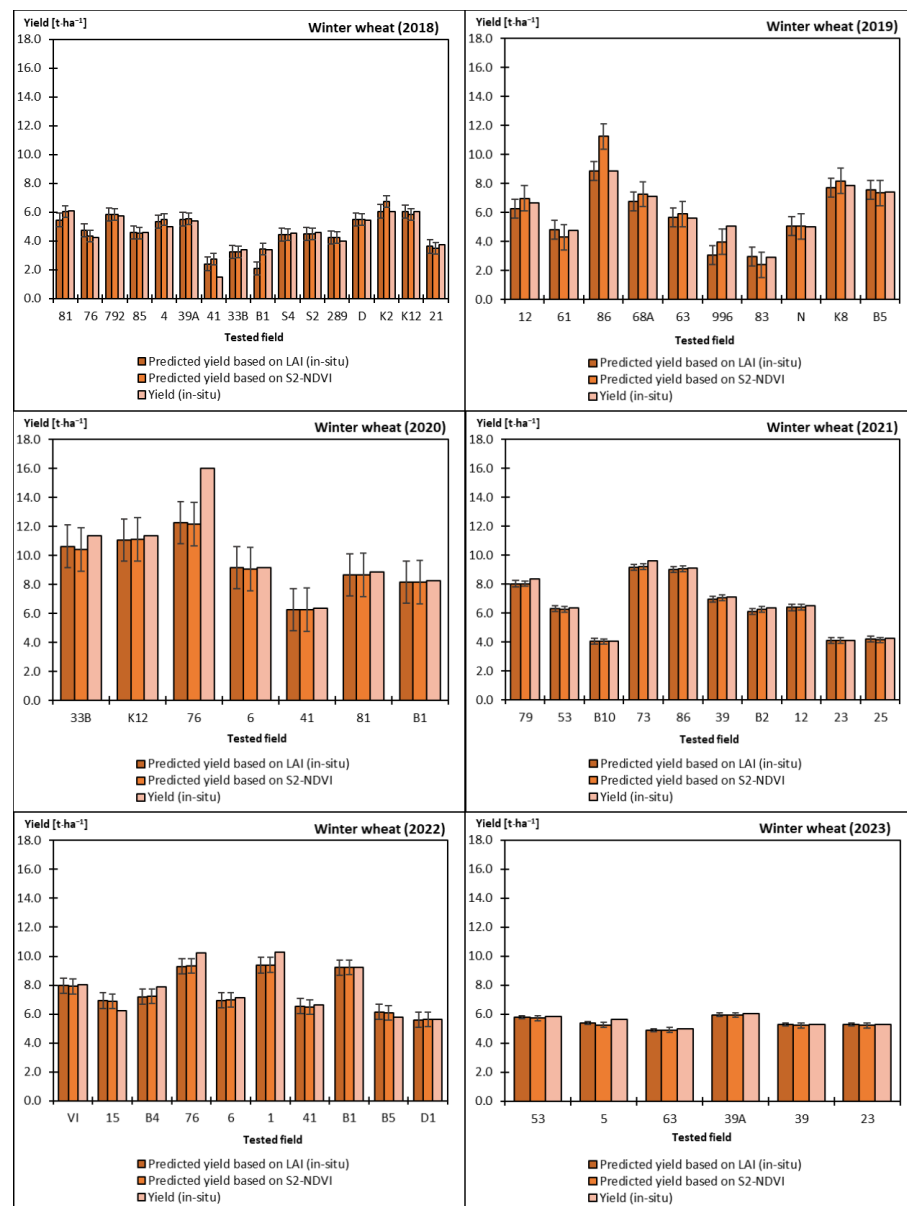


Figure 4. In-situ LAI and NDVI data based on observed and projected yields for the winter wheat crop type from 2018 to 2023.

Table 2. Comparison of model results based on in-situ and satellite data for winter wheat cultivation.

Year	Yield ($t \cdot ha^{-1}$)					
	RMSE ($t \cdot ha^{-1}$)		MAE		MAPE	
	LAI	NDVI	LAI	NDVI	LAI	NDVI
2018	0.463	0.399	0.294	0.252	9.412	8.732
2019	0.898	0.871	0.646	0.564	10.918	9.845
2020	1.453	1.501	0.744	0.787	5.411	5.776
2021	0.201	0.192	0.162	0.137	2.163	1.847
2022	0.531	0.513	0.404	0.390	5.058	4.846
2023	0.106	0.169	0.033	0.049	0.624	2.333

Table 2 presents the statistical analysis of in-situ yield values and simulation results obtained from the in-situ LAI and NDVI data for winter wheat. The research indicates that the ground-based LAI results yield higher error values compared to those based on satellite-derived NDVI, a trend observed for four out of six studied years. This suggests that a predictive model relying on ground-based LAI data may exhibit a relatively limited accuracy compared to a model utilizing satellite-derived NDVI.

3.2. Maize Yield Predictions

This chapter presents the results of the AquaCrop model analysis, utilizing both in-situ data and NDVI satellite data for maize cultivation from 2018 to 2023 (Figure 5).

Upon comparing the results obtained in 2018 with those of other years, it becomes evident that the simulated values, with an RMSE of $0.01 t \cdot ha^{-1}$, closely align with the measured values, indicating a high level of precision in the output. However, simulation results for the years 2020 and 2023 suggest less reliable outcomes with RMSE values of $0.48 t \cdot ha^{-1}$ and $0.75 t \cdot ha^{-1}$, respectively, compared to other years. Conversely, the results for 2019 and 2021, with RMSE values of $0.21 t \cdot ha^{-1}$ and $0.09 t \cdot ha^{-1}$, respectively, adhere to the criteria necessary for considering the model successful.

The research indicates (see Table 3) that results based on in-situ LAI data yield higher error values than those based on satellite NDVI. However, this trend is not consistent across all years, as there are instances where the RMSE values for LAI are lower than those for NDVI. This suggests that while a predictive model relying on ground-based LAI data may exhibit a relatively limited level of accuracy compared to a model associated with satellite-derived NDVI, the relationship between the two datasets can vary depending on the specific year. Notably, the year 2020 exhibits a significantly higher RMSE compared to other years, indicating an elevated level of forecast errors for that specific year.

Table 3. Comparison of model results based on in-situ and satellite data for maize cultivation.

Year	Yield ($t \cdot ha^{-1}$)					
	RMSE ($t \cdot ha^{-1}$)		MAE		MAPE	
	LAI	NDVI	LAI	NDVI	LAI	NDVI
2018	0.011	0.056	0.011	0.056	0.212	1.039
2019	0.210	0.198	0.210	0.198	4.319	4.073
2020	0.486	0.428	0.486	0.428	6.674	5.875
2021	0.089	0.333	0.089	0.333	1.214	4.530
2022	0.131	0.311	0.131	0.311	1.917	4.535
2023	0.750	0.642	0.718	0.603	1.514	0.817

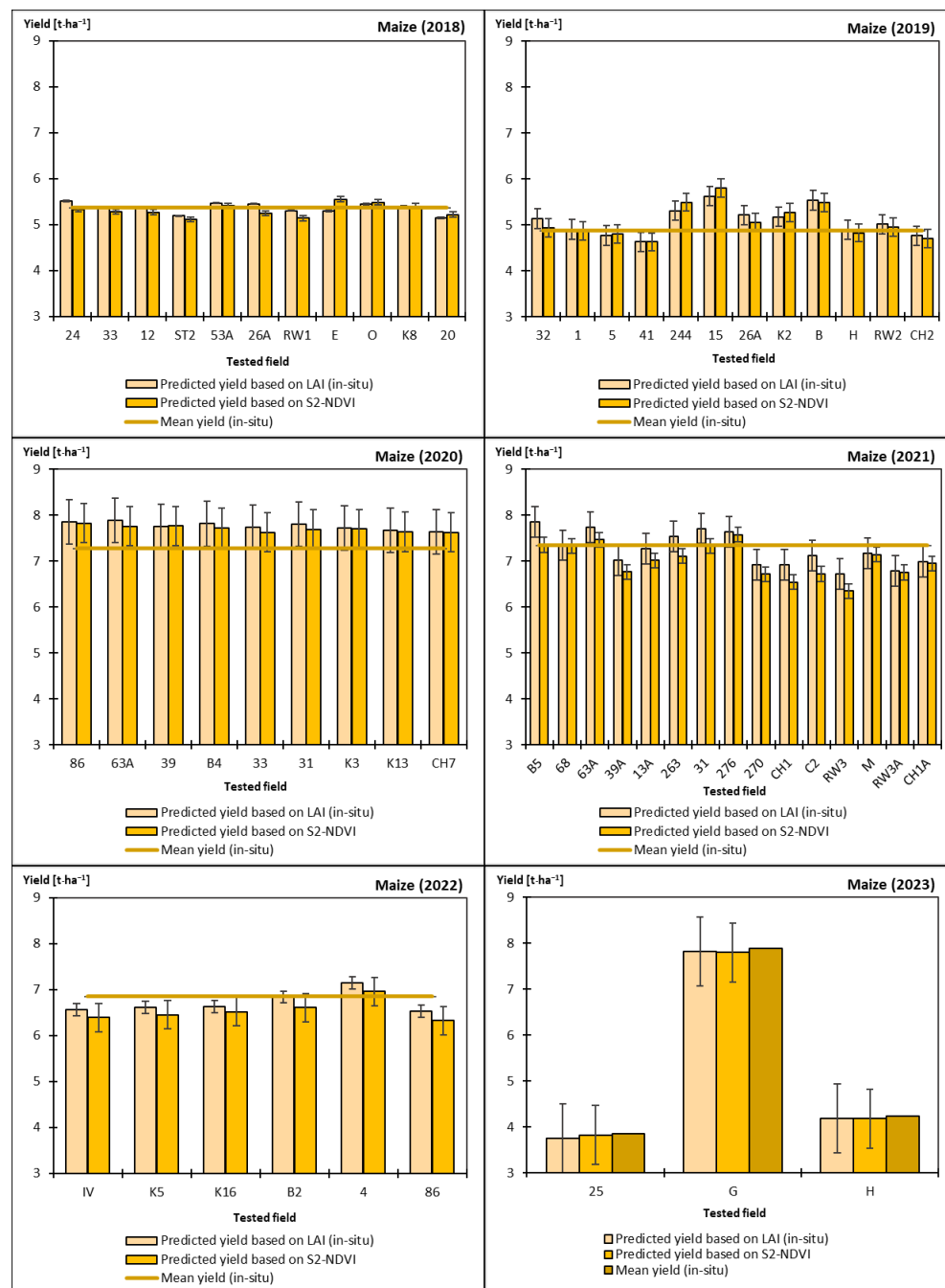


Figure 5. In-situ LAI and NDVI-based on observed and projected yields for the maize crop type in the years 2018 through 2023.

3.3. Winter Rapeseed Yield Predictions

Approaching Figure 6 from a general perspective, it is evident that there exists an average measured value across all years, with estimated values for rapeseed yield prediction closely aligning with this average. Upon closer examination, the RMSE values of 2018 and 2022, at $0.39 \text{ t}\cdot\text{ha}^{-1}$ and $0.23 \text{ t}\cdot\text{ha}^{-1}$, respectively, highlight that the prediction outcomes for these years deviate significantly from the mean measured value, indicating a lower level of reliability compared to the simulation results for other years. Conversely, simulation results for winter rapeseed in the years 2019, 2021, and 2023 demonstrate a remarkable level of precision, with an RMSE value below $0.1 \text{ t}\cdot\text{ha}^{-1}$. These results indicate that the predicted values closely approximate the observed values, showcasing a higher level of reliability compared to other outcomes.

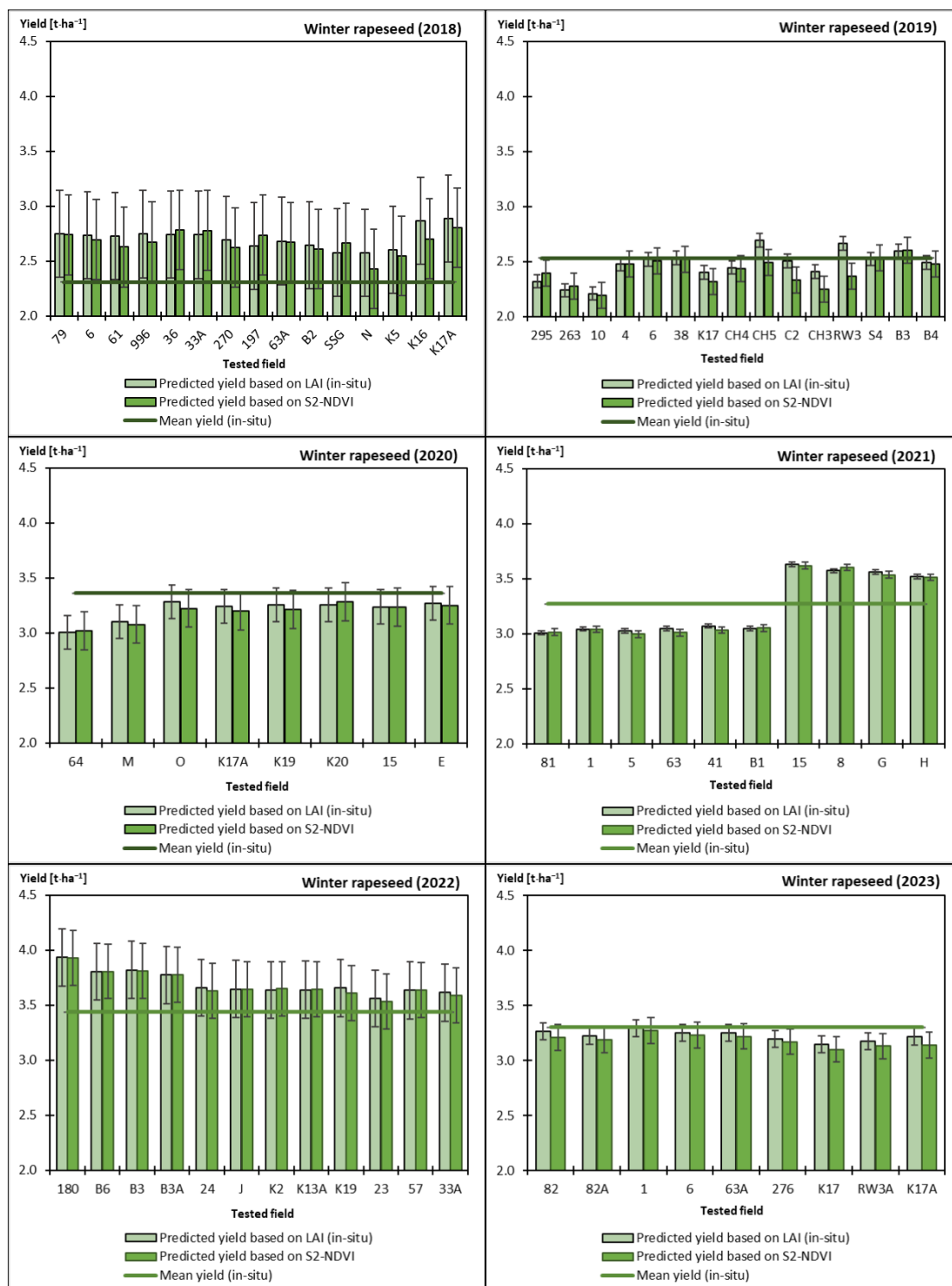


Figure 6. In-situ LAI and NDVI-based data showing observed and projected yields for the winter rapeseed crop from 2018 to 2023.

The validation data, representing actual yields in the studied area, were incorporated as the average winter rapeseed yield in the investigated region (see Table 4). Statistical analysis of the simulation results demonstrates significant convergence. However, results based on the LAI indicator exhibit higher accuracy, albeit not statistically significant. Comparative analysis conducted over the years reveals a gradual trend of predicted values

towards actual values. Notably, when comparing simulation results for different crops, it is observed that the model achieves optimal results for winter rapeseed.

Table 4. Comparison of model results based on in-situ and satellite data in winter rapeseed cultivation.

Year	Yield (t·ha ⁻¹)					
	RMSE (t·ha ⁻¹)		MAE		MAPE	
	LAI	NDVI	LAI	NDVI	LAI	NDVI
2018	0.396	0.363	0.396	0.363	17.149	15.694
2019	0.061	0.118	0.061	0.118	2.430	4.667
2020	0.153	0.172	0.153	0.172	4.561	5.115
2021	0.019	0.029	0.019	0.029	0.578	0.899
2022	0.259	0.249	0.259	0.249	7.524	7.248
2023	0.077	0.116	0.077	0.116	2.330	3.512

3.4. Sugar Beet Yield Predictions

The simulation results for sugar beet cultivation (refer to Figure 7) in 2018 and 2021 indicate a lower level of accuracy, with RMSE values of 0.95 t·ha⁻¹ and 0.78 t·ha⁻¹, respectively. These results suggest a deviation from actual values. However, upon analyzing the simulation results for sugar beet cultivation in 2023, the recorded RMSE value of 0.20 t·ha⁻¹ attests to a high level of accuracy for the predictive model, based on both in-situ measurements and satellite data. This observation underscores the significant ability of the simulation to approximate actual values and, compared to other years, it seems to characterize a higher level of reliability. Examining the simulation results for sugar beet cultivation in the years 2019, 2020, and 2022, the respective RMSE values of 0.61, 0.30, and 0.72 t·ha⁻¹ indicate that the model has achieved the expected predictive precision.

The study demonstrates a consistent downward trend in the analysis results based on LAI over the examined period (Table 5). It is noteworthy that the annual comparison indicates that error values derived from LAI are comparable to those obtained from NDVI, with no consistent trend of one being consistently higher than the other. This suggests that the predictive model associated with LAI may exhibit similar accuracy compared to the NDVI-based model.

Table 5. Comparison of model results based on in-situ and satellite data for sugar beet cultivation.

Year	Yield (t·ha ⁻¹)					
	RMSE (t·ha ⁻¹)		MAE		MAPE	
	LAI	NDVI	LAI	NDVI	LAI	NDVI
2018	0.954	0.872	0.954	0.872	1.653	1.510
2019	0.612	0.613	0.612	0.613	1.079	1.081
2020	0.306	0.402	0.306	0.402	0.489	0.642
2021	0.789	0.673	0.789	0.673	1.277	1.089
2022	0.725	0.632	0.725	0.632	1.125	0.980
2023	0.265	0.298	0.257	0.289	0.453	0.508

This visual representation illuminates the significant potential of using high-resolution satellite data in enhancing the predictability and management of crop yields within the dynamic agricultural landscape of Wielkopolska, particularly amidst the challenges brought forth by climate change. The results reveal a distinct advantage in utilizing satellite data for predicting yields of specific crops such as wheat and sugar beets. Conversely, the analysis across other crops like winter rapeseed and maize demonstrates a remarkable consistency in prediction errors, underscoring the widespread applicability and promise of satellite data in agricultural yield forecasting. This consistency across various crop types suggests that the integration of satellite data into yield forecasting models is not only feasible, but also

holds substantial promise for improving agricultural outcomes across a broad spectrum of practices.

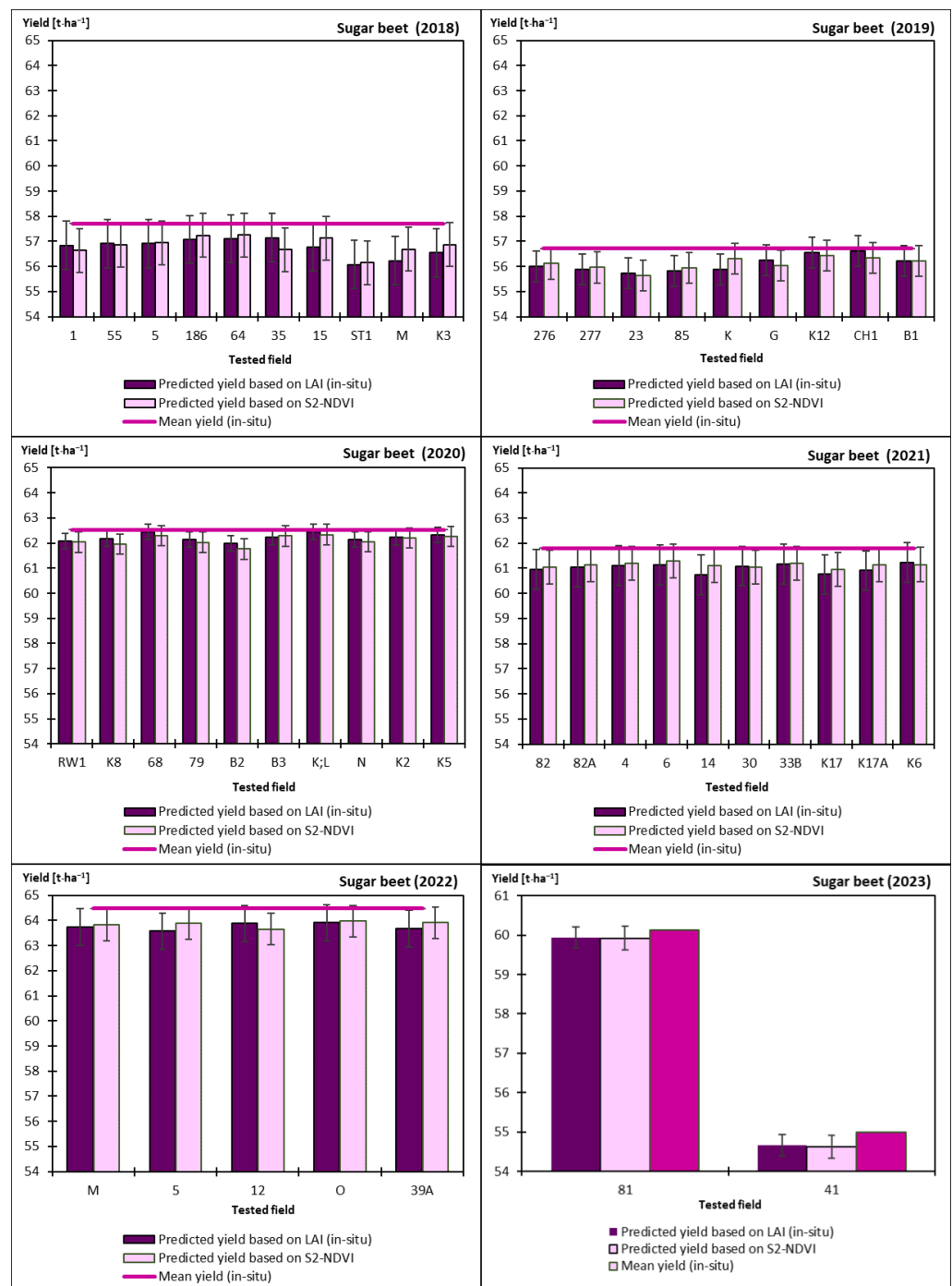


Figure 7. In-situ LAI and NDVI-based on observed and projected yields for the sugar beet crop type from 2018 to 2023.

4. Discussion

Wielkopolska stands out as one of the most significant agricultural regions in Poland. The region’s importance in agriculture underscores the crucial need for monitoring and evaluating crop growth to ensure sustainability, especially in light of dynamic environmental conditions. This study provides a tool for understanding and predicting crop performance in Wielkopolska’s agricultural region through a monitoring system. The

study demonstrates that by utilizing not only on-site collected data but also high-resolution satellite data, the process can be made more efficient in the territory of Poland. This, in turn, shows that agricultural practices can be effectively planned and managed.

For winter wheat, the LAI-based RMSE value is determined as $0.46 \text{ t}\cdot\text{ha}^{-1}$, while the NDVI-based RMSE value is $0.40 \text{ t}\cdot\text{ha}^{-1}$. Additionally, two other studies in the literature have conducted similar measurements for winter wheat yield predictions. In Kale and Madenoglu's 2009–2010 study in Turkey, conducted due to the impact of varying drought events on rain-dependent winter wheat farming, the RMSE value was determined to be $0.32 \text{ t}\cdot\text{ha}^{-1}$ [27]. Saab et al., in their study in Lebanon between 2017 and 2019, integrated the canopy cover fraction derived from Copernicus-Sentinel 2 satellite data into the AquaCrop model to simulate the yield of winter wheat. The results show that the RMSE for yield ranged between 0.34 and $0.42 \text{ t}\cdot\text{ha}^{-1}$ after integration [28].

According to the findings obtained for the maize crop, the LAI-based RMSE value is determined as $0.01 \text{ t}\cdot\text{ha}^{-1}$ while the NDVI-based RMSE value is $0.06 \text{ t}\cdot\text{ha}^{-1}$. In a study conducted by Umesh et al. in Telangana, India, for the years 2013–2014, which investigated the impact of climate change on maize agriculture and examined the effects of additional irrigation, an RMSE value ranging from 0.06 to $0.12 \text{ t}\cdot\text{ha}^{-1}$ was identified [29]. In the study conducted by Mibulo and Kiggundu in Uganda for the years 2014–2015, aiming to increase production in rainfed agricultural systems, predictions made using the AquaCrop model revealed an RMSE value of $0.11 \text{ t}\cdot\text{ha}^{-1}$. These findings indicate that studies conducted under different agricultural conditions encounter similar levels of prediction errors [30]. When examining the sample studies, a slight difference is observed. However, upon reviewing studies conducted by Umesh et al., the presence of various applications such as irrigation treatments, sub-treatments (no mulching and mulching), and two sub-sub-treatments (namely, normal fertilizer and high fertilizer) for maize might suggest that the differences in outcomes could be attributed to these divergent approaches. Upon reviewing the studies of Mibulo and Kiggundu, the observed difference is believed to stem from various factors within their studies, including pests, fertility, and management. These factors have been overlooked in our study.

For sugar beet cultivation, LAI-based RMSE was determined to be $0.95 \text{ t}\cdot\text{ha}^{-1}$, while the NDVI-based RMSE was found to be $0.87 \text{ t}\cdot\text{ha}^{-1}$ for the year 2018, representing the highest values achieved. Garcia-Vila et al. conducted a study in 2012 and 2014 to calibrate and validate the AquaCrop model for sugar beet. They aimed to assess crop responses to varying irrigation levels and evaluate yield and water efficiency across different irrigation water allocations in two main sugar beet production areas in Spain, covering both spring and autumn cultivation seasons. Based on the performance results, AquaCrop demonstrated a high level of accuracy, with an RMSE of $0.85 \text{ t}\cdot\text{ha}^{-1}$ when simulating the final yield [31]. Similarly, Stricevic et al. studied the period 2000–2007 in Serbia, addressing the necessity of irrigation due to frequent drought occurrences in the region, and they reported an RMSE value of $0.03 \text{ t}\cdot\text{ha}^{-1}$ [32]. The likely explanation for the higher RMSE value compared to the other two studies could be the variation in fields allocated for sugar beet cultivation each year. This suggests that differences in the datasets may also contribute to these outcomes.

For winter rapeseed, the LAI-based RMSE value was determined to be $0.40 \text{ t}\cdot\text{ha}^{-1}$, while the NDVI-based RMSE value was found to be $0.36 \text{ t}\cdot\text{ha}^{-1}$ in 2018, representing the year with the highest observed values for these errors. The research conducted by Mousavizadeh et al. from 2005 to 2008 in Iran aimed to simulate real conditions where water stress could be applied during various growth periods of winter rapeseed. The precision of the model they formulated was ascertained, yielding an RMSE value of $0.92 \text{ t}\cdot\text{ha}^{-1}$ for crop yield [33]. The influence of severe water stress conditions was overlooked in this study, whereas the inclusion of this parameter in the researchers' investigation might account for the disparities in findings. Particularly, the significant impact of severe water stress throughout the entire growth cycle, facilitated by supplementary irrigation, could substantially affect the accuracy of predictions.

While our study has provided valuable insights into crop yield prediction using the AquaCrop model and satellite data, it is essential to acknowledge certain limitations. Firstly, the accuracy of predictions may be influenced by factors such as soil heterogeneity, which was not extensively accounted for in our modeling approach. Additionally, while satellite data offer valuable information, they may not capture certain micro-level variations in crop conditions, leading to potential discrepancies between predicted and observed yields. Furthermore, the calibration and validation of the AquaCrop model rely on historical data, which may not fully account for future changes in climate patterns or agricultural practices. Moreover, the transferability of our findings to other regions or crops should be approached with caution, as agricultural systems vary widely in their environmental and management contexts. Future research could focus on refining the model to incorporate more dynamic factors, such as real-time climate data and pest or disease outbreaks, to enhance prediction accuracy and robustness. However, it is crucial to also consider alternative approaches, such as the utilization of gridded data, as suggested by Liakopoulou and Mavromatis (2023) [34], which could offer valuable insights in crop simulation modeling.

5. Conclusions

The integration of the AquaCrop model with satellite data proves to be a useful tool for forecasting crop yields in the JECAM fields of Wielkopolska from 2018 to 2023. This model's strength lies in its ability to finely adjust predictions to local soil conditions and management factors, significantly contributing to the optimization of agricultural processes.

The utilization of satellite data, particularly NDVI, facilitates the monitoring of vegetation changes, providing valuable insights into plant health and biomass quantity. AquaCrop, calibrated based on Leaf Area Index (LAI) data, consistently generates coherent yield predictions, offering a foundation for more precise crop planning and effective resource management.

Results from extensive statistical analyses indicate a decreasing trend in error indicators across the four crop types, suggesting a gradual improvement in the predictive accuracy of the model over the studied six-year period. However, it is essential to note that this conclusion is based on a relatively limited dataset. Further studies covering additional years are necessary in order to validate and maintain conclusions regarding the observed trend.

Furthermore, the findings of this study contribute significantly to the existing body of knowledge in agricultural management by demonstrating the effectiveness of integrating advanced modeling techniques with satellite data for crop yield forecasting. By leveraging high-resolution satellite imagery and ground-based measurements, this research enhances our understanding of crop growth dynamics and provides valuable insights into optimizing agricultural practices. This improved predictive accuracy of the AquaCrop model, coupled with satellite data, not only aids in better crop planning and resource allocation, but also lays the groundwork for implementing precision agriculture strategies. Thus, this study not only addresses the immediate needs of agricultural management in the Wielkopolska region, but also serves as a valuable reference for similar agricultural systems globally.

Author Contributions: Conceptualization, K.D.-Z.; methodology, E.P.-C.; software, E.P.-C. and C.N.O.; validation, E.P.-C. and C.N.O.; formal analysis, E.P.-C.; investigation, E.P.-C.; resources, E.P.-C.; data curation, E.P.-C., C.N.O. and R.G.; writing—original draft, E.P.-C. and C.N.O.; writing—review and editing, E.P.-C. and K.D.-Z.; visualization, C.N.O.; supervision, K.D.-Z.; project administration, K.D.-Z.; funding acquisition, K.D.-Z. All authors have read and agreed to the published version of the manuscript.

Funding: The research work was conducted within the project financed by the National Centre for Research and Development under Contract No. PLRPA/02/SAPOL4Crop/43/2018, titled "SA Polish collaborative crop growth monitoring and yield assessment system for early warning utilizing new satellite Earth Observations data from Copernicus Programme". This work was supported by The National Centre for Research and Development within the program "POLNOR 2019 call"

Project: “Tools for information to farmers on grasslands yields under stressed conditions to support management practices” (2020–2023).

Data Availability Statement: Data will be made available upon request.

Acknowledgments: We extend our heartfelt thanks to the entire team at the Remote Sensing Centre for their invaluable ground measurements conducted from 2018 to 2023. Additionally, we appreciate the significant contributions of our colleagues at the Agricultural Research Council from South Africa for their expertise in knowledge exchange related to crop assessment.

Conflicts of Interest: The authors declare no conflicts of interest.

References

1. Choryński, A.; Pińskwar, I.; Graczyk, D.; Krzyżaniak, M. The Emergence of Different Local Resilience Arrangements Regarding Extreme Weather Events in Small Municipalities—A Case Study from the Wielkopolska Region, Poland. *Sustainability* **2022**, *14*, 2052. [\[CrossRef\]](#)
2. Szwed, M. Projections of Changes of Areal Evapotranspiration for Different Land-Use Units in the Wielkopolska Region (Poland). *Theor. Appl. Climatol.* **2017**, *130*, 291–304. [\[CrossRef\]](#)
3. Goliński, P.; Czerwiński, M.; Jørgensen, M.; Mølmann, J.A.B.; Golińska, B.; Taff, G. Relationship between Climate Trends and Grassland Yield across Contrasting European Locations. *Open Life Sci.* **2018**, *13*, 589–598. [\[CrossRef\]](#) [\[PubMed\]](#)
4. Panek, E.; Gozdowski, D.; Stępień, M.; Samborski, S.; Ruciński, D.; Buszke, B. Within-Field Relationships between Satellite-Derived Vegetation Indices, Grain Yield and Spike Number of Winter Wheat and Triticale. *Agronomy* **2020**, *10*, 1842. [\[CrossRef\]](#)
5. Panek, E.; Gozdowski, D. Relationship between MODIS Derived NDVI and Yield of Cereals for Selected European Countries. *Agronomy* **2021**, *11*, 340. [\[CrossRef\]](#)
6. Panek-Chwastyk, E.; Dąbrowska-Zielińska, K.; Kluczek, M.; Markowska, A.; Woźniak, E.; Bartold, M.; Ruciński, M.; Wojtkowski, C.; Aleksandrowicz, S.; Gromny, E.; et al. Estimates of Crop Yield Anomalies for 2022 in Ukraine Based on Copernicus Sentinel-1, Sentinel-3 Satellite Data, and ERA-5 Agrometeorological Indicators. *Sensors* **2024**, *24*, 2257. [\[CrossRef\]](#) [\[PubMed\]](#)
7. Gozdowski, D.; Stępień, M.; Panek, E.; Varghese, J.; Bodecka, E.; Rozbicki, J.; Samborski, S. Comparison of Winter Wheat NDVI Data Derived from Landsat 8 and Active Optical Sensor at Field Scale. *Remote Sens. Appl. Soc. Environ.* **2020**, *20*, 100409. [\[CrossRef\]](#)
8. Dąbrowska-Zielinska, K.; Kogan, F.; Ciolkosz, A.; Gruszczynska, M.; Kowalik, W. Modelling of Crop Growth Conditions and Crop Yield in Poland Using AVHRR-Based Indices. *Int. J. Remote Sens.* **2002**, *23*, 1109–1123. [\[CrossRef\]](#)
9. Iqbal, M.A.; Shen, Y.; Stricevic, R.; Pei, H.; Sun, H.; Amiri, E.; Penas, A.; Del Rio, S. Evaluation of the FAO AquaCrop Model for Winter Wheat on the North China Plain under Deficit Irrigation from Field Experiment to Regional Yield Simulation. *Agric. Water Manag.* **2014**, *135*, 61–72. [\[CrossRef\]](#)
10. Beyhan, Y.D.; Candoğan, B.N. FAO AquaCrop Modeli Kullanılarak Farklı Sulama Programı Koşullarında Patates Bitkisinde Verim Tahmini. *Çomü Ziraat Fakültesi Derg.* **2019**, *7*, 91–98. [\[CrossRef\]](#)
11. Linker, R.; Ioslovich, I. Assimilation of Canopy Cover and Biomass Measurements in the Crop Model AquaCrop. *Biosyst. Eng.* **2017**, *162*, 57–66. [\[CrossRef\]](#)
12. Cheng, M.; Wang, H.; Fan, J.; Xiang, Y.; Liu, X.; Liao, Z.; Abdelghany, A.E.; Zhang, F.; Li, Z. Evaluation of AquaCrop Model for Greenhouse Cherry Tomato with Plastic Film Mulch under Various Water and Nitrogen Supplies. *Agric. Water Manag.* **2022**, *274*, 107949. [\[CrossRef\]](#)
13. Wellens, J.; Raes, D.; Fereres, E.; Diels, J.; Coppys, C.; Adiele, J.G.; Ezui, K.S.G.; Becerra, L.-A.; Selvaraj, M.G.; Dercon, G.; et al. Calibration and Validation of the FAO AquaCrop Water Productivity Model for Cassava (*Manihot esculenta* Crantz). *Agric. Water Manag.* **2022**, *263*, 107491. [\[CrossRef\]](#)
14. Trombetta, A.; Iacobellis, V.; Tarantino, E.; Gentile, F. Calibration of the AquaCrop Model for Winter Wheat Using MODIS LAI Images. *Agric. Water Manag.* **2016**, *164*, 304–316. [\[CrossRef\]](#)
15. Er-Raki, S.; Bouras, E.; Rodriguez, J.C.; Watts, C.J.; Lizarraga-Celaya, C.; Chehbouni, A. Parameterization of the AquaCrop Model for Simulating Table Grapes Growth and Water Productivity in an Arid Region of Mexico. *Agric. Water Manag.* **2021**, *245*, 106585. [\[CrossRef\]](#)
16. Maniruzzaman, M.; Talukder, M.S.U.; Khan, M.H.; Biswas, J.C.; Nemes, A. Validation of the AquaCrop Model for Irrigated Rice Production under Varied Water Regimes in Bangladesh. *Agric. Water Manag.* **2015**, *159*, 331–340. [\[CrossRef\]](#)
17. Coudron, W.; Gobin, A.; Boeckeaert, C.; De Cuyper, T.; Lootens, P.; Pollet, S.; Verheyen, K.; De Frenne, P.; De Swaef, T. Data Collection Design for Calibration of Crop Models Using Practical Identifiability Analysis. *Comput. Electron. Agric.* **2021**, *190*, 106457. [\[CrossRef\]](#)
18. Li, F.; Yu, D.; Zhao, Y. Irrigation Scheduling Optimization for Cotton Based on the AquaCrop Model. *Water Resour. Manag.* **2019**, *33*, 39–55. [\[CrossRef\]](#)
19. Mbangiwa, N.C.; Savage, M.J.; Mabhaudhi, T. Modelling and Measurement of Water Productivity and Total Evaporation in a Dryland Soybean Crop. *Agric. For. Meteorol.* **2019**, *266–267*, 65–72. [\[CrossRef\]](#)
20. De Roos, S.; De Lannoy, G.J.M.; Raes, D. Performance Analysis of Regional AquaCrop (v6.1) Biomass and Surface Soil Moisture Simulations Using Satellite and in Situ Observations. *Biogeosciences* **2021**, *2021*, 1–23. [\[CrossRef\]](#)

21. Mejias, P.; Piraux, M. *AquaCrop, the Crop Water Productivity Model*; Food and Agriculture Organization of the United Nations: Rome, Italy, 2017; Volume 4.
22. Zhang, T.; Zuo, Q.; Ma, N.; Shi, J.; Fan, Y.; Wu, X.; Wang, L.; Xue, X.; Ben-Gal, A. Optimizing Relative Root-Zone Water Depletion Thresholds to Maximize Yield and Water Productivity of Winter Wheat Using AquaCrop. *Agric. Water Manag.* **2023**, *286*, 108391. [[CrossRef](#)]
23. Raes, D. *AquaCrop Training Handbook I. Understanding AquaCrop August 2023*; Food and Agriculture Organization of the United Nations: Rome, Italy, 2023.
24. Raes, D.; Steduto, P.; Hsiao, T.C.; Fereres, E. Reference Manual, Chapter 3. In *AquaCrop, Version 7.0—August 2022*; Food and Agriculture Organization of the United Nations: Rome, Italy, 2023.
25. Van Gaelen, H.; Tsegay, A.; Delbecque, N.; Shrestha, N.; Garcia, M.; Fajardo, H.; Miranda, R.; Vanuytrecht, E.; Abrha, B.; Diels, J.; et al. A Semi-Quantitative Approach for Modelling Crop Response to Soil Fertility: Evaluation of the AquaCrop Procedure. *J. Agric. Sci.* **2015**, *153*, 1218–1233. [[CrossRef](#)]
26. Alvar-Beltrán, J.; Saturnin, C.; Grégoire, B.; Camacho, J.L.; Dao, A.; Migraine, J.B.; Marta, A.D. Using AquaCrop as a Decision-Support Tool for Improved Irrigation Management in the Sahel Region. *Agric. Water Manag.* **2023**, *287*, 108430. [[CrossRef](#)]
27. Kale, S.; Madenoğlu, S. Evaluating AquaCrop Model for Winter Wheat under Various Irrigation Conditions in Turkey. *Tarım Bilim. Derg.* **2018**, *24*, 205–217. [[CrossRef](#)]
28. Abi Saab, M.T.; El Alam, R.; Jomaa, I.; Skaf, S.; Fahed, S.; Albrizio, R.; Todorovic, M. Coupling Remote Sensing Data and AquaCrop Model for Simulation of Winter Wheat Growth under Rainfed and Irrigated Conditions in a Mediterranean Environment. *Agronomy* **2021**, *11*, 2265. [[CrossRef](#)]
29. Umesh, B.; Reddy, K.S.; Poligowdar, B.S.; Maruthi, V.; Satishkumar, U.; Ayyanagoudar, M.S.; Rao, S.; Veeresh, H. Assessment of Climate Change Impact on Maize (*Zea mays* L.) through Aquacrop Model in Semi-Arid Alfisol of Southern Telangana. *Agric. Water Manag.* **2022**, *274*, 107950. [[CrossRef](#)]
30. Mibulo, T.; Kiggundu, N. Evaluation of FAO AquaCrop Model for Simulating Rainfed Maize Growth and Yields in Uganda. *Agronomy* **2018**, *8*, 238. [[CrossRef](#)]
31. Garcia-Vila, M.; Morillo-Velarde, R.; Fereres, E. Modeling Sugar Beet Responses to Irrigation with AquaCrop for Optimizing Water Allocation. *Water* **2019**, *11*, 1918. [[CrossRef](#)]
32. Stricevic, R.; Cosic, M.; Djurovic, N.; Pejic, B.; Maksimovic, L. Assessment of the FAO AquaCrop Model in the Simulation of Rainfed and Supplementally Irrigated Maize, Sugar Beet and Sunflower. *Agric. Water Manag.* **2011**, *98*, 1615–1621. [[CrossRef](#)]
33. Mousavizadeh, S.F.; Honar, T.; Ahmadi, S.H. Assessment of the AquaCrop Model for Simulating Canola under Different Irrigation Managements in a Semiarid Area. *Int. J. Plant Prod.* **2016**, *10*, 425–445.
34. Liakopoulou, K.S.; Mavromatis, T. Evaluation of Gridded Meteorological Data for Crop Sensitivity Assessment to Temperature Changes: An Application with CERES-Wheat in the Mediterranean Basin. *Climate* **2023**, *11*, 180. [[CrossRef](#)]

Disclaimer/Publisher’s Note: The statements, opinions and data contained in all publications are solely those of the individual author(s) and contributor(s) and not of MDPI and/or the editor(s). MDPI and/or the editor(s) disclaim responsibility for any injury to people or property resulting from any ideas, methods, instructions or products referred to in the content.